

# Co2PO: Coordinated Constrained Policy Optimization for Multi-Agent RL

Shrenik Patel <sup>†1</sup> Christine Truong <sup>†2</sup>

## Abstract

Constrained multi-agent reinforcement learning (MARL) faces a fundamental tension between exploration and safety-constrained optimization. Existing leading approaches, such as Lagrangian methods, typically rely on global penalties or centralized critics that react to violations after they occur, often suppressing exploration and leading to over-conservatism. We propose Co2PO, a novel MARL communication-augmented framework that enables coordination-driven safety through selective, risk-aware communication. Co2PO introduces a shared blackboard architecture for broadcasting positional intent and yield signals, governed by a learned hazard predictor that proactively forecasts potential violations over an extended temporal horizon. By integrating these forecasts into a constrained optimization objective, Co2PO allows agents to anticipate and navigate collective hazards without the performance trade-offs inherent in traditional reactive constraints. We evaluate Co2PO across a suite of complex multi-agent safety benchmarks, where it achieves higher returns compared to leading constrained baselines while converging to cost-compliant policies at deployment. Ablation studies further validate the necessity of risk-triggered communication, adaptive gating, and shared memory components.

## 1. Introduction

Constrained multi-agent reinforcement learning (MARL) aims to maximize collective return while satisfying safety constraints, but in cooperative settings this tension is especially sharp: aggressive exploration can incur costly violations, while overly conservative updates can prematurely suppress learning and prevent agents from discovering high-

<sup>†</sup>Equal contribution <sup>1</sup>Rutgers University, New Brunswick, NJ  
<sup>2</sup>Carnegie Mellon University, Pittsburgh, PA. Correspondence to: Shrenik Patel <shrenik.patel@rutgers.edu>, Christine Truong <cmtruong@andrew.cmu.edu>.

Preprint. February 4, 2026.

performing joint behavior (Brunke et al., 2022). The problem is amplified by partial observability and interaction-driven dynamics. Even when agents share the same reward objective, safety failures often emerge from coordination breakdowns in timing, intent, or mutual awareness, rather than from conflicting incentives (Omidshafiei et al., 2015; Calzolari et al., 2026). As a result, purely reactive constraint handling can be slow to correct the underlying cause of violations, while heavy-handed penalties can make learning brittle (Brunke et al., 2022).

We introduce Co2PO, a coordinated constrained policy optimization framework that targets these coordination-driven safety failures through *selective, risk-aware coordination*. Rather than treating communication as a persistent channel, Co2PO uses it as a sparse control mechanism: agents write to a shared blackboard only when they predict elevated near-term hazard risk. Each write contains compact safety-relevant signals—a positional state summary, an intent vector, and a yield flag—that other agents can retrieve to condition their actions. This design preserves decentralized action selection while providing coordination signals precisely when interaction risk is most acute.

Across cooperative multi-agent safety benchmarks, Co2PO improves feasible performance and reaches cost-compliant policies at evaluation under the same training budget. We observe transient violations early in training, when hazard prediction and coordination behavior are still being learned, but final policies satisfy the cost constraint during evaluation. Our contributions are as follows:

## Contributions.

- We introduce Co2PO, enabling selective coordination via a shared blackboard with decentralized actions.
- We propose hazard-triggered writes of compact signals (state, intent, yield) with adaptive write-rate control.
- We evaluate on cooperative multi-agent safety benchmarks with ablations isolating blackboard and gating.

## 2. Problem Setup and Preliminaries

We study constrained cooperative multi-agent reinforcement learning (MARL) under partial observability. Agents seek high return while satisfying an expected cost budget at eval-

uation, and we summarize performance with *feasible return*.

## 2.1. Constrained Cooperative Markov Game

We model the environment as a cooperative constrained Markov game (CMG) with  $n$  agents (Littman, 1994):

$$\mathcal{G} = \langle \mathcal{N}, \mathcal{S}, \{\mathcal{O}_i\}_{i \in \mathcal{N}}, \{\mathcal{A}_i\}_{i \in \mathcal{N}}, P, r, c, \gamma, \rho_0, d \rangle.$$

Agent  $i$  observes  $o_t^i \in \mathcal{O}_i$  and selects  $a_t^i \in \mathcal{A}_i$ , yielding joint action  $a_t = (a_1^1, \dots, a_t^n)$  and transition  $s_{t+1} \sim P(\cdot | s_t, a_t)$  from  $s_0 \sim \rho_0$ . The environment emits a shared reward  $r_t = r(s_t, a_t)$  and safety cost  $c_t = c(s_t, a_t)$ .

Policies factorize as  $\pi(a | o) = \prod_{i=1}^n \pi_i(a^i | o^i)$  with  $o = (o^1, \dots, o^n)$ . The discounted return and cost are

$$J_R(\pi) = \mathbb{E}_\pi \left[ \sum_{t=0}^{\infty} \gamma^t r(s_t, a_t) \right], \quad (1)$$

$$J_C(\pi) = \mathbb{E}_\pi \left[ \sum_{t=0}^{\infty} \gamma^t \bar{c}(s_t, a_t) \right], \quad (2)$$

where  $\bar{c}$  is the team cost used for enforcement. We seek

$$\max_{\pi} J_R(\pi) \quad \text{s.t.} \quad J_C(\pi) \leq d, \quad (3)$$

with cost budget  $d$ .

## 2.2. CTDE Preliminaries

We use centralized training with decentralized execution (CTDE): critics may condition on centralized information during training, while each actor  $\pi_i$  conditions only on its local observation (and any permitted message/memory) at execution (Lowe et al., 2020; Yu et al., 2022).

## 2.3. Safety Metric: Feasible Return

We report *feasible return* to reflect deployment-time cost constraints:

$$J_F(\pi) = J_R(\pi) \cdot \mathbf{1}[J_C(\pi) \leq d]. \quad (4)$$

## 2.4. Lagrangian Relaxation

We optimize a Lagrangian relaxation of Equation (3), following standard constrained policy optimization formulations (Achiam et al., 2017):

$$\max_{\pi} \min_{\lambda \geq 0} \mathcal{L}(\pi, \lambda) = J_R(\pi) - \lambda(J_C(\pi) - d), \quad (5)$$

with the dual variable  $\lambda$  updated online. Actor-critic updates commonly use a hybrid advantage (Tessler et al., 2018; Ray et al., 2019; Zhang et al., 2020)

$$A_t^{\text{hyb}} = A_t^R - \lambda A_t^C. \quad (6)$$

## 2.5. Risk Events and Hazard Labels

We construct a proactive hazard label from dense per-step costs. Let  $c_t^i$  be the instantaneous cost for agent  $i$ . Define a hazard event

$$z_t^i = \mathbf{1}[c_t^i > \delta], \quad (7)$$

and a lookahead label with horizon  $H$ ,

$$h_t^i = \mathbf{1}\left[\max_{\tau \in \{t, \dots, t+H\}} z_\tau^i = 1\right], \quad (8)$$

computed within episode boundaries. We use  $h_t^i$  to supervise the hazard predictor used for selective coordination in Section 3.

## 3. Methodology

We present Co2PO, a constrained MARL method that augments decentralized policies with *selective* shared-memory coordination. Each agent predicts near-term hazard risk from its local observation and writes a compact message to a shared blackboard only when predicted risk exceeds a threshold. Agents then read a fixed-size context from the blackboard and condition their actions on the retrieved information. Training uses a constrained actor-critic objective with reward and cost critics, a dual variable for constraint enforcement, supervised hazard forecasting, and a penalty that discourages excessive writing.

### 3.1. Per-Timestep Interaction Protocol

We consider  $E$  parallel environment instances and  $n$  agents. At timestep  $t$  in environment  $e$ : (1) *write-info* each agent computes hazard probability and message contents from its observation; (2) *write* agents gate writes and update the blackboard; (3) *read* each agent retrieves up to  $k$  other agents' messages to form a fixed-length context; (4) *act* each agent selects an action conditioned on its observation and retrieved context. The blackboard is maintained per environment instance and cleared on episode termination.

### 3.2. Blackboard: State, Write, and Read

**Stored fields.** For each environment  $e$  and agent  $i$ , the blackboard stores a single current entry

$$B_t^{e,i} = (x_t^{e,i}, u_t^{e,i}, y_t^{e,i}, p_t^{e,i}, w_t^{e,i}), \quad (9)$$

where  $x_t^{e,i} \in \mathbb{R}^d$  is a compact state summary,  $u_t^{e,i} \in \mathbb{R}^d$  is a learned intent vector,  $y_t^{e,i} \in [0, 1]$  is a learned yield flag,  $p_t^{e,i} \in [0, 1]$  is the hazard probability, and  $w_t^{e,i} \in \{0, 1\}$  is the write indicator.

**Write information from local observation.** Each agent computes message fields and a hazard score from its observation:

$$(\ell_t^i, u_t^i, y_t^i) = F_\theta(o_t^i), \quad p_t^i = \sigma(\ell_t^i), \quad (10)$$

where  $\ell_t^i$  is a hazard logit and  $\sigma(\cdot)$  is the sigmoid.

**Event-triggered writes.** Writes are gated by a threshold:

$$w_t^{e,i} = \mathbf{1}[p_t^{e,i} > \tau_t], \quad (11)$$

and only entries with  $w_t^{e,i} = 1$  are valid for reads.

#### Similarity-based read (top- $k$ ) with fixed-length context.

At each timestep, agent  $i$  forms a query vector from its own state summary,  $q_t^{e,i} = x_t^{e,i}$ . It then considers the set of *active* entries written by other agents in the same environment instance,  $\{B_t^{e,j} : j \neq i, w_t^{e,j} = 1\}$ , and scores each candidate  $j$  by cosine similarity (Das et al., 2020):

$$s_t^e(i, j) = \left\langle \frac{x_t^{e,j}}{\|x_t^{e,j}\|_2 + \varepsilon}, \frac{q_t^{e,i}}{\|q_t^{e,i}\|_2 + \varepsilon} \right\rangle,$$

where  $\varepsilon > 0$  is a small constant for numerical stability. Agent  $i$  retrieves the  $k$  highest-scoring active entries and, for each retrieved sender  $j$ , constructs

$$\psi(B_t^{e,j}) = [x_t^{e,j}; u_t^{e,j}; y_t^{e,j}; p_t^{e,j}] \in \mathbb{R}^{2d+2}.$$

The memory context is the concatenation of up to  $k$  such vectors in ranked order, zero-padded if fewer than  $k$  entries are active:

$$m_t^{e,i} = [\psi(B_t^{e,j_1}); \dots; \psi(B_t^{e,j_k})] \in \mathbb{R}^{k(2d+2)}. \quad (12)$$

#### 3.3. Threshold Control (Optional)

We allow adaptation of  $\tau_t$  online to target a desired write rate  $\rho^*$ . Let  $\rho_t$  be the observed mean write rate and  $\bar{\rho}_t$  its exponential moving average (Stooke & Abbeel, 2020):

$$\bar{\rho}_t = \beta \bar{\rho}_{t-1} + (1 - \beta) \rho_t, \quad (13)$$

$$\tau_{t+1} = \text{clip}\left(\tau_t + \eta(\bar{\rho}_t - \rho^*), \tau_{\min}, \tau_{\max}\right), \quad (14)$$

where  $\beta \in (0, 1)$ , step size  $\eta > 0$ , and bounds  $(\tau_{\min}, \tau_{\max})$  prevent degenerate write thresholds.

#### 3.4. Policy and Critics

**Memory-conditioned decentralized actor.** Each actor conditions on its observation and the retrieved context:

$$a_t^i \sim \pi_{\phi_i}(\cdot | o_t^i, \text{enc}(m_t^i)), \quad (15)$$

where  $\text{enc}(\cdot)$  maps Equation (12) to an embedding concatenated with  $o_t^i$ .

**Centralized critics.** Under CTDE, we learn reward and cost critics  $V^R(\cdot)$  and  $V^C(\cdot)$  to compute reward and cost advantages for policy optimization.

#### 3.5. Learning Objective

**Constrained policy optimization.** We optimize the Lagrangian objective (Equation (5)) using a hybrid advantage  $A_t^{\text{hyb},i} = A_t^{R,i} - \lambda A_t^{C,i}$ , with  $\lambda \geq 0$  updated by projected primal-dual learning.

**Actor loss.** Let  $r_t^i(\phi_i)$  denote the importance ratio between current and behavior policies. We use a clipped surrogate objective augmented with hazard supervision and a write penalty (Schulman et al., 2017):

$$\begin{aligned} \mathcal{L}_{\text{actor}}^i &= \mathcal{L}_{\text{clip}}^i(A^{\text{hyb},i}) + \alpha_{\text{write}} \mathbb{E}[w_t^i] \\ &\quad + \alpha_{\text{haz}} \mathbb{E}[\text{WBCE}(\ell_t^i, h_t^i)] - \alpha_{\text{ent}} \mathcal{H}(\pi_{\phi_i}). \end{aligned} \quad (16)$$

Here WBCE is weighted binary cross-entropy,  $\mathcal{H}$  is policy entropy, and  $\alpha_{\text{write}}, \alpha_{\text{haz}}, \alpha_{\text{ent}} \geq 0$  are coefficients.

**Hazard supervision, critics, and dual update.** We supervise the hazard head with the lookahead label  $h_t^i$  (Section 2.5). Reward and cost critics are trained by value regression to their respective returns, and the dual variable  $\lambda$  is updated via a projected step driven by observed constraint violations.

#### 3.6. Algorithm

**Algorithm 1** Co2PO: one rollout step at timestep  $t$  (for all envs  $e$  and agents  $i$ ).

- 1: **Write-info:** compute  $(\ell_t^{e,i}, p_t^{e,i}, u_t^{e,i}, y_t^{e,i})$  from  $o_t^{e,i}$  for all  $(e, i)$
- 2: **Gate & write:** set  $w_t^{e,i} \leftarrow \mathbf{1}[p_t^{e,i} > \tau_t]$  and update blackboard entries  $B_t^{e,i}$
- 3: **Adapt:** optionally update  $\tau_t$  using Equations (13) and (14)
- 4: **Read:** for each  $(e, i)$ , form  $m_t^{e,i}$  by top- $k$  retrieval from active entries (Equation (12))
- 5: **Act:** sample  $a_t^{e,i} \sim \pi_{\phi_i}(\cdot | o_t^{e,i}, \text{enc}(m_t^{e,i}))$  and step environments
- 6: **Store:** add transitions (including  $m_t^{e,i}$  and  $w_t^{e,i}$ ) to buffer; clear blackboard for terminated envs

## 4. Experimental Setup

### 4.1. Benchmarks

We evaluate on cooperative multi-agent safety benchmarks from the SAFEPPO suite, which builds on SAFETY-GYMNASIUM and provides a consistent multi-agent interface (Ji et al., 2024). Each task emits a per-step reward and safety cost; our goal is to maximize return while meeting an episodic cost budget.

**Velocity family.** In multi-agent velocity tasks, agents must coordinate to achieve velocity-tracking objectives while avoiding unsafe behavior under task-specific safety costs (Todorov et al., 2012). These tasks are coordination-stressing because agents share a space: one agent’s behavior can perturb others’ motion, making it harder to maintain target speeds without constraint violations.

**MultiGoal family.** In multi-agent MultiGoal tasks, agents navigate shared spaces with safety costs arising from unsafe states or contacts (e.g., hazards) (Ji et al., 2024). They stress partial observability, interaction-driven hazards, and implicit negotiation to remain cost-compliant.

## 4.2. Baselines

We compare against constrained MARL baselines implemented in SAFEPO: *MAPPO* (Yu et al., 2022), *HAPPO* (Kuba et al., 2022), *MACPO* (Gu et al., 2023), and *MAPPO-Lagrangian* (Gu et al., 2023). All methods are run under a matched training budget and evaluation protocol. When available, we use SAFEPO’s standard hyperparameter configurations for each baseline and environment to avoid unfair retuning. All hyperparameters for all methods (including method-specific settings) are reported in Appendix D for reproducibility.

## 4.3. Metrics

Let an episode have horizon  $T$  with  $n$  agents. Following the SAFEPO convention, we aggregate reward and cost across agents by averaging per-step signals over agents and summing over time:

$$R = \sum_{t=0}^{T-1} \frac{1}{n} \sum_{i=1}^n r_t^i, \quad C = \sum_{t=0}^{T-1} \frac{1}{n} \sum_{i=1}^n c_t^i. \quad (17)$$

We evaluate policies at checkpoints  $t \in \mathcal{T}$  during training; let  $\hat{R}_t$ ,  $\hat{C}_t$  denote mean episodic return/cost over evaluation episodes at checkpoint  $t$ . We report:

- **Final return/cost** ( $R_{\text{final}}$ ,  $C_{\text{final}}$ ):  $\hat{R}_{t_{\text{last}}}$  and  $\hat{C}_{t_{\text{last}}}$  at the last checkpoint  $t_{\text{last}}$ .
- **Peak cost** ( $C_{\text{peak}}$ ):  $\max_{t \in \mathcal{T}} \hat{C}_t$ , capturing the worst evaluated cost over training.
- **Violation rate**: fraction of evaluation episodes whose episodic cost exceeds the budget  $d$  (i.e.,  $\Pr[C > d]$ ).
- **Feasible return** ( $R_{\text{feas}}$ ): best evaluation return among checkpoints that satisfy the cost budget,

$$R_{\text{feas}} = \max_{t \in \mathcal{T}} \left\{ \hat{R}_t : \hat{C}_t \leq d \right\}. \quad (18)$$

- **Time-to-feasible**: the earliest training step corresponding to a checkpoint  $t$  with  $\hat{C}_t \leq d$ ; if no checkpoint is feasible, we report “–”.

## 4.4. Training and Evaluation Protocol

We follow the standard SAFEPO on-policy training loop: collect rollouts with  $E$  parallel environment instances, perform multiple epochs of minibatch updates per iteration, and periodically evaluate the current policy in separate evaluation rollouts (Ji et al., 2024). Evaluation uses deterministic action selection and reports means ( $\pm$  standard deviation) over three independent random seeds.

## 5. Results

We evaluate Co2PO on coordination-intensive environments under constrained multi-agent learning. Across all settings, Co2PO achieves higher feasible returns than leading baselines while maintaining evaluation-time cost compliance at convergence. To facilitate comparison across heterogeneous tasks, we aggregate feasible performance and evaluation-time cost by environment type.

*Table 1.* Mean feasible return across Velocity and Multi-goal environments, and mean final evaluation cost for Velocity tasks.

Method	$R_{\text{feas}}$ (Vel.)	$R_{\text{feas}}$ (Multi.)	$C_{\text{final}}$ (Vel.)
MAPPO	866	3.38	525.34
MAPPO-Lag	1593	7.09	1.54
MACPO	738	0.69	6.94
HAPPO	1023	13.00	536.05
<b>Co2PO</b>	<b>1709</b>	<b>10.00</b>	<b>12.30</b>

### 5.1. Feasible Performance Under Safety Constraints

Co2PO consistently identifies higher-quality feasible solutions throughout training. Across velocity-based environments, Co2PO achieves a mean feasible-return improvement of approximately 7% relative to MAPPO-Lag, with a median improvement of 7% (Table 1). These gains are consistent across all velocity tasks, ranging from 6.5% to 7.9% depending on the environment.

In the coordination-intensive multi-goal environment with a feasible region, Co2PO achieves an absolute feasible-return improvement of 2.91 over MAPPO-Lag (see Appendix A for all per-environment statistics). Although the percentage gains are inflated by small baseline values, the absolute improvement confirms Co2PO’s effectiveness in coordination-heavy regimes.

Co2PO demonstrates consistent deployment readiness on the Velocity family: final evaluation costs stabilize across seeds, and cost-compliant checkpoints are reliably reached while maintaining strong returns. In all MultiGoal settings, no method reaches the cost budget within the training horizon, so we focus on return–cost tradeoffs rather than feasible return (Section 6).

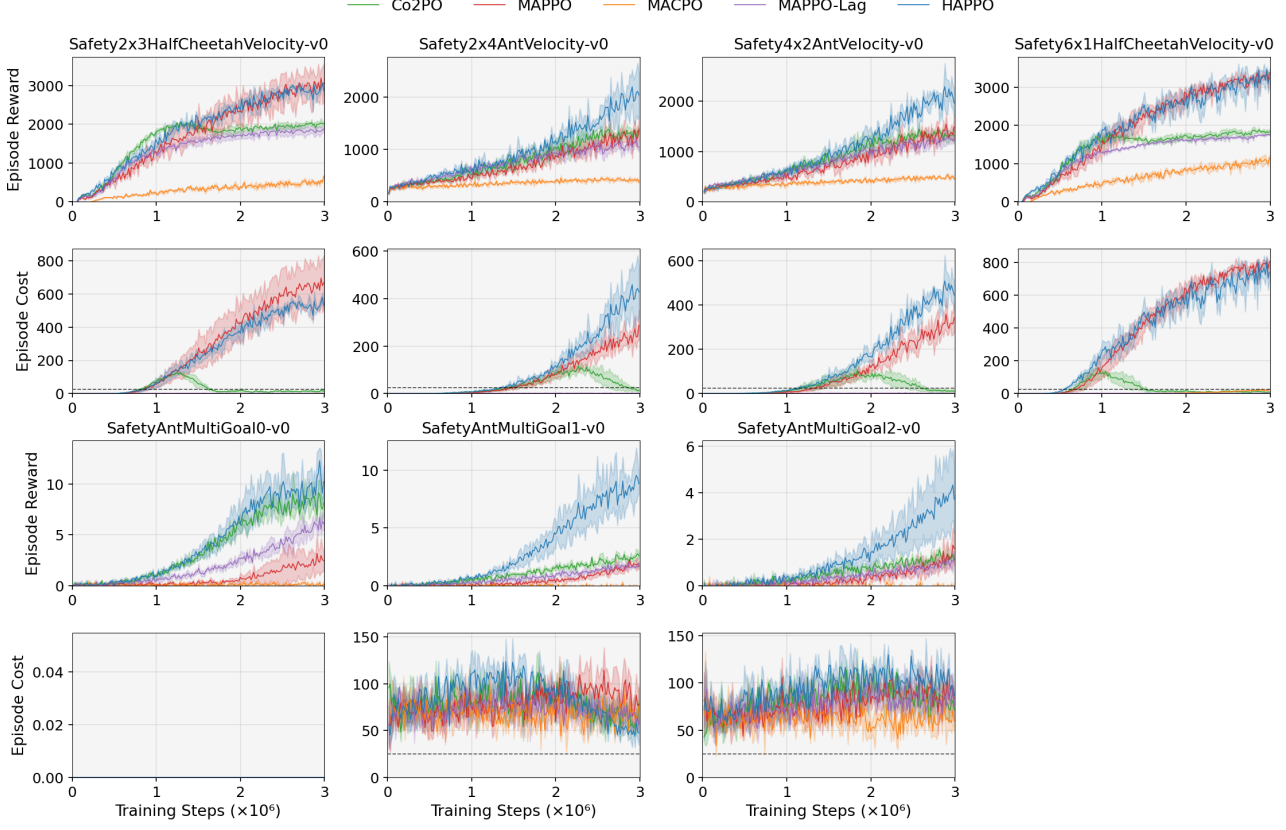


Figure 1. Results on seven SAFEPPO cooperative safety benchmarks. We report both evaluation return and cost.

## 5.2. Learning Dynamics and Exploration–Safety Tradeoff

Table 2. Mean early return and peak episodic cost for velocity environments.

Method	$C_{\text{peak}}$ (Vel.)	$R_{\text{early}}$ (Vel.)
MAPPO	855	1023
MAPPO-Lag	2	881
MACPO	79	622
HAPPO	792	1124
<b>Co2PO</b>	<b>231</b>	<b>1221</b>

Peak episodic cost  $C_{\text{peak}}$  characterizes worst-case constraint violations during training and highlights differences in exploration behavior. Co2PO permits bounded early violations, incurring higher peak cost than conservative constrained baselines while remaining substantially below unconstrained methods (Table 2). This behavior is confined to early training and reflects an intentional relaxation of constraint enforcement to promote exploration.

This relaxation enables faster reward acquisition. Over the first  $10^6$  environment steps, Co2PO achieves higher early evaluation return than MAPPO-Lag and MACPO, indicating more rapid learning progress under partial observability. In

contrast, methods that aggressively suppress early violations exhibit lower peak cost but slower reward growth and ultimately converge to lower feasible return (Section 5.1). By tolerating transient violations while enforcing constraints at convergence, Co2PO accelerates learning toward higher-quality, deployable policies.

## 5.3. Deployment Safety and Stability

We evaluate deployment safety using final evaluation cost  $C_{\text{final}}$  and violation statistics at convergence. Across velocity environments, Co2PO exhibits stable and bounded cost behavior at evaluation time, with low variation across tasks (coefficient of variation,  $\text{CV} \approx 0.20$ ), indicating predictable deployment performance. This stability is comparable to that of constrained baselines (MAPPO-Lag  $\text{CV} \approx 0.29$ , MACPO  $\text{CV} \approx 1.53$ ), showing that Co2PO’s constraint satisfaction generalizes consistently across environments.

Safety constraint satisfaction at convergence is consistent, with a mean standard deviation of approximately 8% across velocity environments. Final costs remain within a feasible range (mean  $C_{\text{final}} = 12.30$ , range 8.85–15.17), indicating reliable constraint enforcement without erratic cost dynamics. The low cost variance, bounded violations, and reli-

able feasibility attainment indicate that Co2PO’s constraint satisfaction at convergence is consistent and suitable for deployment, rather than brittle or noise-sensitive.

#### 5.4. Environment-Dependent Behavioral Patterns

Co2PO’s performance varies systematically with coordination demands. The largest improvements occur in environments requiring explicit multi-agent coordination, such as ANTVEL, where Co2PO achieves substantially higher feasible return and more reliable constraint satisfaction than constrained baselines ( $R_{\text{feas}} \approx 1,450$  vs.  $\approx 1,350$  for MAPPO-Lag across ANTVEL environments; Appendix A). In these settings, reactive and unconstrained baselines frequently fail to converge to compliant solutions within the training horizon: MAPPO and HAPPO do not achieve feasibility in all of the environments, including HALFCHEETAHVEL variants.

In contrast, environments with simpler dynamics and weaker inter-agent coupling, such as single-direction HALFCHEETAHVEL variants, exhibit more modest but consistent gains ( $R_{\text{feas}} \approx 1,950$  vs.  $\approx 1,850$ ), while maintaining comparable stability at convergence. A similar trend appears in multi-goal environments, where Co2PO yields large relative improvements (approximately 40% over MAPPO-Lag; Appendix A). Overall, Co2PO’s benefits are environment-dependent rather than uniform, scaling with coordination demands while generalizing across diverse tasks.

#### 5.5. Comparative Safety–Performance Analysis

The evaluated baselines exhibit distinct safety–performance tradeoffs. Unconstrained methods such as HAPPO and MAPPO achieve high returns but incur substantial costs and elevated violation rates. MAPPO-Lag reliably enforces constraints but converges to overly conservative policies, resulting in markedly reduced feasible return. MACPO occupies an intermediate regime, mitigating some violations while allowing limited exploration, but consistently underperforms Co2PO across all evaluated environments.

Co2PO differs by enabling proactive constraint enforcement. Through hazard prediction and selective inter-agent communication, Co2PO permits controlled early exploration without sacrificing constraint satisfaction at convergence. This yields a consistently improved safety–performance tradeoff, combining both higher feasible return and reliable deployment-time safety.

Overall, these results suggest that coupling selective coordination with predicted risk provides a practical mechanism for balancing exploration and constraint satisfaction. Importantly, Co2PO’s gains do not stem from constraint enforcement alone, but from improved coordination efficiency that allows agents to reach higher feasible returns.

## 6. Ablations

We ablate Co2PO’s coordination components to isolate which mechanisms drive improvements in feasible performance. We focus on three representative environments that span fast locomotion with interaction-driven hazards (HALFCHEETAHVEL, ANTVEL) and a harder navigation-and-coordination setting (ANTMULTIGOAL). All ablations keep the same training budget and settings as the full method. We additionally study the effect of the hazard lookahead horizon in Appendix B.

**Takeaway.** Figure 3 and Table 3 shows that removing either (i) shared-memory coordination (*w/o Blackboard*) or (ii) selective gating (*Always-Write*) reduces feasible performance on the Velocity tasks. The most pronounced degradation occurs when removing hazard supervision (*w/o Hazard Loss*), which substantially worsens both feasibility and performance in ANTVEL.

### 6.1. Shared Memory Is Beneficial for Feasible Performance

**w/o Blackboard** removes inter-agent shared context, while keeping the rest of training unchanged. On HALFCHEETAHVEL and ANTVEL, this consistently lowers feasible return relative to Co2PO (e.g., 2054 → 1907 on HALFCHEETAHVEL and 1468 → 1365 on ANTVEL), indicating that the blackboard context is contributing useful coordination information beyond what is recoverable from local observations alone. Final evaluation costs remain below budget in these Velocity settings, suggesting the main effect of removing the blackboard is reduced *feasible performance* rather than purely increased constraint violations.

In ANTMULTIGOAL, none of the compared methods reaches the budget within the plotted horizon; we therefore report final return instead of feasible return. Here, removing the blackboard increases  $R_{\text{final}}$  but also increases  $C_{\text{final}}$  (Table 3), highlighting that this environment exhibits a different trade-off regime where constraint satisfaction is not yet achieved by any method in the training budget we consider.

### 6.2. Selective Writes Matter

**Always-Write** disables sparsity by forcing all agents to write every timestep, while keeping the same message format and read mechanism. Across the Velocity tasks, Always-Write underperforms the full method in feasible return (e.g., 2054 → 1915 on HALFCHEETAHVEL and 1468 → 1284 on ANTVEL), with final costs that remain broadly comparable. This supports the practical motivation for selective coordination: indiscriminate writing does not reliably improve feasible performance under a fixed training budget, and can introduce additional noise into the retrieved context.

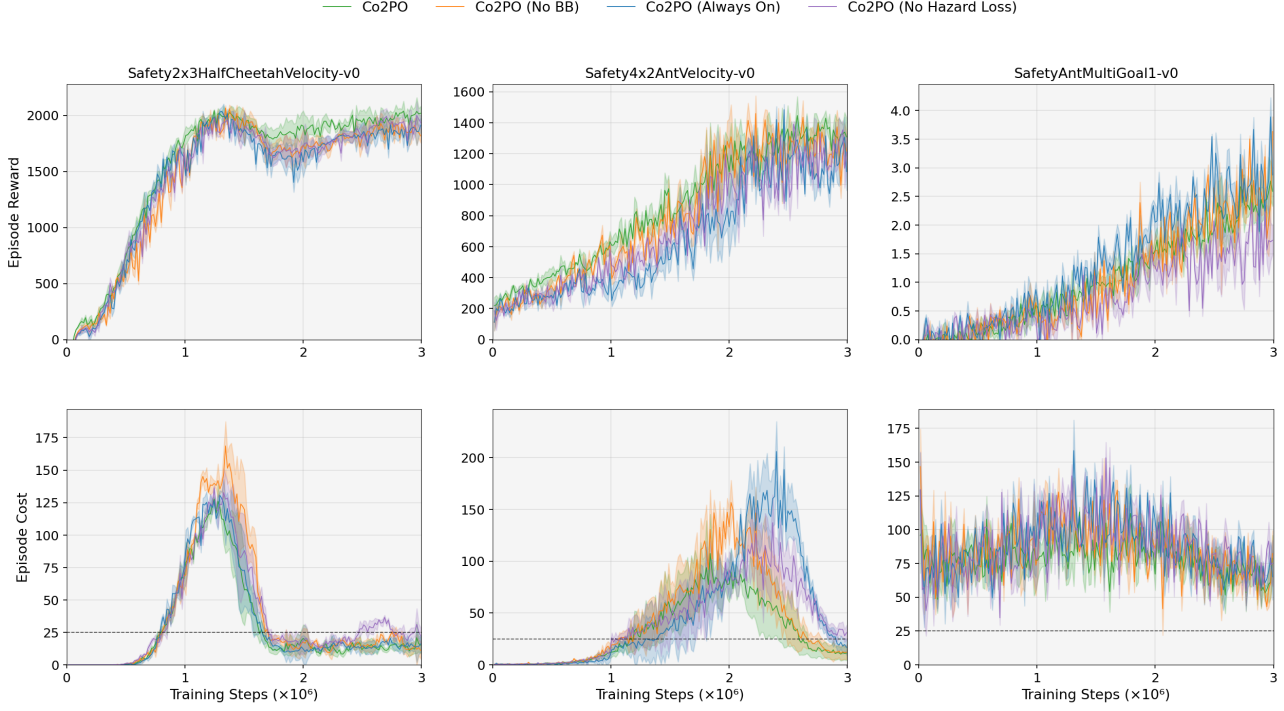


Figure 2. Ablations on three environments. We report both evaluation return and cost.

Table 3. **Ablation summary.** For Velocity tasks we report *feasible return* and the final evaluation cost  $C_{\text{final}}$  at the last checkpoint. For ANTMULTIGOAL, no method reaches the budget within the plotted horizon, so we report final return  $R_{\text{final}}$  instead.

<b>Method</b>	HalfCheetahVel		AntVel		AntMultiGoal	
	$R_{\text{feas}} \uparrow$	$C_{\text{final}} \downarrow$	$R_{\text{feas}} \uparrow$	$C_{\text{final}} \downarrow$	$R_{\text{final}} \uparrow$	$C_{\text{final}} \downarrow$
Co2PO	$2054 \pm 70$	$15.2 \pm 7.9$	$1468 \pm 43$	$11.3 \pm 8.8$	$2.59 \pm 0.32$	$78.8 \pm 20.8$
Co2PO w/o Blackboard	$1907 \pm 65$	$12.3 \pm 6.4$	$1365 \pm 40$	$13.7 \pm 10.6$	$3.46 \pm 0.42$	$84.4 \pm 22.3$
Co2PO (Always-Write)	$1915 \pm 65$	$16.6 \pm 8.6$	$1284 \pm 38$	$14.9 \pm 11.6$	$3.07 \pm 0.38$	$67.0 \pm 17.7$
Co2PO w/o Hazard Loss	$1936 \pm 66$	$23.1 \pm 12.0$	$566 \pm 17$	$28.2 \pm 21.9$	$1.98 \pm 0.24$	$74.6 \pm 19.7$

On ANTMULTIGOAL, Always-Write yields a lower final cost than the full method but does not resolve infeasibility; all variants remain above the budget. We treat this setting as a stress test as none of the baselines reach compliance with regard to the set cost target.

### 6.3. Hazard Supervision Is Important for Feasibility

**w/o Hazard Loss** removes explicit supervision of the hazard predictor while leaving the coordination pathway intact. This ablation has the most severe impact on ANTVEL: feasible return collapses ( $1468 \rightarrow 566$ ) and final cost rises above the budget ( $11.3 \rightarrow 28.2$ ). The learning curves in Figure 3 are consistent with the intuition that without direct hazard learning signal, the write trigger becomes less aligned with safety-relevant events, reducing the effectiveness of selective coordination and degrading constraint satisfaction.

On HALFCHEETAHVEL, the same ablation increases final

cost while still remaining under budget on average (Table 3), and yields a modest drop in feasible return relative to the full method. On ANTMULTIGOAL, removing hazard supervision decreases final return without materially changing the overall infeasibility regime.

## 7. Related Work

**Constrained Reinforcement Learning.** Constrained reinforcement learning (CRL) addresses policy optimization under explicit safety, resource, or performance constraints, most commonly via Lagrangian relaxation that embeds costs into the objective through adaptive penalty coefficients (Zhang et al., 2019). Single-agent methods such as CPO (Achiam et al., 2017), PPO with Lagrangian relaxation (Ray et al., 2019), and FOCOPS (Zhang et al., 2020) enforce constraints in expectation, but are often sensitive to penalty tuning and rely on reactive updates that correct violations only after they occur, which can slow learning or induce conserva-

tive behavior (Stooke & Abbeel, 2020). Extensions to multi-agent settings adopt similar principles, employing centralized critics or shared multipliers (e.g., MAPPO-Lagrangian and MACPO) to enforce global constraints. While effective at reducing violations, these approaches largely rely on reactive, penalty-based constraint handling and can suppress exploration in coordination-intensive environments.

**Safe Multi-Agent Reinforcement Learning.** Safe multi-agent reinforcement learning (Safe MARL) further considers cooperative settings where safety violations arise from collective interactions rather than isolated actions. Most safe MARL methods operate under the centralized training with decentralized execution (CTDE) paradigm and augment standard MARL backbones such as MAPPO with global cost critics or shared constraint signals (Hernandez-Leal et al., 2019; Foerster et al., 2024), rather than value-factorization approaches such as QMIX (Sunehag et al., 2017; Rashid et al., 2018). However, safety is typically enforced through aggregated penalties that provide limited guidance for resolving coordination-induced violations, leading to slow learning dynamics or overly conservative policies (Gu et al., 2023). Prior work in hierarchical MARL demonstrates that explicit coordination improves task performance, suggesting that similar mechanisms may be beneficial for safety-constrained multi-agent settings.

**Communication and Memory in MARL.** Communication has been widely studied as a means of improving coordination in MARL, particularly under partial observability, through message passing or graph-based information sharing (Sukhbaatar et al., 2016; Kim et al., 2019; Das et al., 2020; Jiang et al., 2020). Existing approaches primarily use communication to enhance task performance and learning stability (Peng et al., 2021; Calzolari et al., 2026), without explicitly targeting safety constraints. Some methods combine communication with safety mechanisms by coupling MAPPO-style training with execution-time safety filters or shields (Alshiekh et al., 2017), while others incorporate shared cost signals during training to enforce constraints. In both cases, safety is handled reactively via centralized penalties or post-hoc intervention, and communication is rarely conditioned on anticipated risk or collective hazard.

Co2PO departs from prior work by coupling communication with safety objectives as part of the learning process, rather than engineering safety as an external rule. In addition to Lagrangian constraint penalties, Co2PO leverages hazard prediction to selectively trigger communication and coordination when safety risks are anticipated. Communication is neither constant nor purely performance-driven, but explicitly conditioned on predicted constraint violations, allowing more targeted and efficient safety coordination.

## 8. Discussion

**Why Co2PO helps.** Our central hypothesis is that many safety failures in cooperative MARL are *coordination-induced*: violations arise from mismatched timing, intent, or mutual awareness under partial observability. Co2PO addresses this by turning communication into a *risk-triggered control signal*. Agents only broadcast when their hazard predictor anticipates near-term risk, and the blackboard carries compact, safety-relevant semantics (state summary, intent, yield, hazard probability) that other agents can immediately condition on. This differs from purely reactive constraint handling, where penalties increase *after* violations and can suppress exploration globally (Brunke et al., 2022; Gu et al., 2023).

**Empirical takeaways.** Across seven SAFEPO benchmarks, Co2PO consistently finds higher-quality feasible checkpoints than strong constrained baselines, especially on the Velocity family where interaction-driven hazards are common (Figure 1). The learning curves also reflect an explicit exploration–safety strategy: Co2PO tolerates bounded early violations (higher  $C_{\text{peak}}$ ) to acquire reward faster, then improves constraint satisfaction and stabilizes by deployment (Section 5). Ablations isolate the key mechanisms, justifying the role of the blackboard, selective writes, and hazard supervision (Figure 3 and Table 3). In the appendix, varying the lookahead horizon further supports the role of proactive labeling as nonzero horizons can improve the return–cost tradeoff relative to  $H=0$  (Section B).

**Limitations and future work.** First, Co2PO is designed to target *deployment-safe policies under a fixed training budget*, rather than zero-violation training-time safety (Alshiekh et al., 2017; Berkenkamp et al., 2017): peak violations can be larger than conservative baselines, which may be unacceptable in some real systems. Second, our hazard labels rely on dense per-step costs and a hand-chosen threshold  $\delta$  (and horizon  $H$ ), which may not be available or stable across domains; learning hazard signals from sparse events, uncertainty-aware predictors, or model-based rollouts is a natural extension (Yang et al., 2020; Calzolari et al., 2026). Third, the Multi-Goal regime remains challenging under our fixed budget, suggesting we need training signals that better reflect delayed coordination effects (e.g., when early yielding prevents later conflicts). Finally, we have not yet stressed scalability: blackboard retrieval and message semantics may need compression, structured routing, or graph-based selection as agent counts grow (Goeckner et al., 2024). Together, these directions would broaden Co2PO’s applicability and improve robustness of risk-triggered coordination across domains, horizons, and agent scales.

## Impact Statement

This work advances methods for learning policies under safety constraints in multi-agent environments. Improved constrained MARL can reduce unsafe behavior in high-stakes domains where multiple decision-makers interact. Potential risks include misuse in adversarial settings or deployment without adequate monitoring; we encourage careful evaluation, transparent reporting of training-time violations, and robust safety testing prior to real-world use.

## References

Achiam, J., Held, D., Tamar, A., and Abbeel, P. Constrained policy optimization, 2017. arXiv:1705.10528.

Alshiekh, M., Bloem, R., Ehlers, R., Könighofer, B., Niekum, S., and Topcu, U. Safe reinforcement learning via shielding, 2017. arXiv:1708.08611.

Berkenkamp, F., Turchetta, M., Schoellig, A. P., and Krause, A. Safe model-based reinforcement learning with stability guarantees, 2017. arXiv:1705.08551.

Brunke, L. et al. Safe learning in robotics: From guarantees to implementations, 2022. arXiv:2108.06266.

Calzolari, G., Sumathy, V., Kanellakis, C., and Nikolakopoulos, G. Safe heterogeneous multi-agent rl with communication regularization for coordinated target acquisition, 2026. arXiv:2601.08327.

Das, A., Gervet, T., Romoff, J., Batra, D., Parikh, D., Rabbat, M., and Pineau, J. Tarmac: Targeted multi-agent communication, 2020. arXiv:1810.11187.

Foerster, J., Farquhar, G., Afouras, T., Nardelli, N., and Whiteson, S. Counterfactual multi-agent policy gradients, 2024. arXiv:1705.08926.

Goeckner, A., Sui, Y., Martinet, N., Li, X., and Zhu, Q. Graph neural network-based multi-agent reinforcement learning for resilient distributed coordination of multi-robot systems, 2024. arXiv:2403.13093.

Gu, Z., Fu, Q., and Dong, H. Safe multi-agent reinforcement learning for multi-robot real-time systems, 2023. arXiv:2110.02793.

Hernandez-Leal, P., Kaisers, M., Baarslag, T., and de Cote, E. M. A survey of learning in multiagent environments: Dealing with non-stationarity, 2019. arXiv:1707.09183.

Ji, J., Zhang, B., Zhou, J., Pan, X., Huang, W., Sun, R., Geng, Y., Zhong, Y., Dai, J., and Yang, Y. Safety-gymnasium: A unified safe reinforcement learning benchmark, 2024. arXiv:2310.12567.

Jiang, J., Dun, C., Huang, T., and Lu, Z. Graph convolutional reinforcement learning, 2020. arXiv:1810.09202.

Kim, J., Park, J., Kim, Y., and Park, S. Learning to schedule communication in multi-agent reinforcement learning, 2019. arXiv:1902.01554.

Kuba, J., Jiang, Y., Wei, W., and Hao, J. Trust region multi-agent policy optimization, 2022. arXiv:2109.11251.

Littman, M. L. Markov games as a framework for multi-agent reinforcement learning. In *Proceedings of the 11th International Conference on Machine Learning (ICML)*, pp. 157–163, 1994.

Lowe, R., Wu, Y., Tamar, A., Harb, J., Abbeel, P., and Mordatch, I. Multi-agent actor-critic for mixed cooperative-competitive environments, 2020. arXiv:1706.02275.

Omidshafiei, S., akbar Agha-mohammadi, A., Amato, C., and How, J. P. Decentralized control of partially observable markov decision processes using belief space macro-actions, 2015. arXiv:1502.06030.

Peng, Z., Vuong, Q., Amos, B., et al. Coordinated policy optimization, 2021. arXiv:2110.13827.

Rashid, T., Samvelyan, M., de Witt, C. S., Farquhar, G., Foerster, J., and Whiteson, S. Qmix: Monotonic value function factorisation for deep multi-agent reinforcement learning, 2018. arXiv:1803.11485.

Ray, A., Achiam, J., and Amodei, D. Benchmarking safe exploration in deep reinforcement learning, 2019. OpenAI Technical Report.

Schulman, J., Wolski, F., Dhariwal, P., Radford, A., and Klimov, O. Proximal policy optimization algorithms, 2017. arXiv:1707.06347.

Stooke, A. and Abbeel, P. Responsive safety in reinforcement learning by pid lagrangian methods, 2020. arXiv:2007.03964.

Sukhbaatar, S., Szlam, A., and Fergus, R. Learning multiagent communication with backpropagation, 2016. arXiv:1605.07736.

Sunehag, P., Lever, G., Gruslys, A., Czarnecki, W. M., Zambaldi, V., Jaderberg, M., Lanctot, M., Sonnerat, N., Leibo, J. Z., Tuyls, K., and Graepel, T. Value-decomposition networks for cooperative multi-agent learning, 2017. arXiv:1706.05296.

Tessler, C., Mankowitz, D. J., and Mannor, S. Reward constrained policy optimization, 2018. arXiv:1805.11074.

Todorov, E., Erez, T., and Tassa, Y. Mujoco: A physics engine for model-based control. In *2012 IEEE/RSJ International Conference on Intelligent Robots and Systems*, pp. 5026–5033, 2012. doi: 10.1109/IROS.2012.6386109.

Yang, Y., Luo, R., Li, M., Zhou, M., Zhang, W., and Wang, J. Mean field multi-agent reinforcement learning, 2020. arXiv:1802.05438.

Yu, C., Velu, A., Vinitsky, E., Gao, J., Wang, Y., Bayen, A., and Wu, Y. The surprising effectiveness of ppo in cooperative, multi-agent games, 2022. arXiv:2103.01955.

Zhang, K., Yang, Z., and Başar, T. Multi-agent reinforcement learning: A selective overview of theories and algorithms, 2019. arXiv:1911.10635.

Zhang, Y., Vuong, Q., and Ross, K. W. First order constrained optimization in policy space, 2020. arXiv:2002.06506.

## A. Complete Evaluation Metrics

Table 4. Full evaluation metrics aggregated across runs.

Environment	Method	$R_{\text{final}}$	$R_{\text{feas}}$	$C_{\text{final}}$	$C_{\text{peak}}$	Violation rate	Time-to-feasible
Safety2x3HalfCheetahVelocity	MAPPO	3068 $\pm$ 491	1094 $\pm$ 43	667.17 $\pm$ 164.13	712	0.71 $\pm$ 0.02	–
	MAPPO-Lag	1882 $\pm$ 74	1904 $\pm$ 86	1.10 $\pm$ 0.51	3	0.00 $\pm$ 0.00	16000
	MACPO	657 $\pm$ 22	663 $\pm$ 16	0.48 $\pm$ 0.21	0	0.00 $\pm$ 0.00	16000
	HAPPO	2878 $\pm$ 143	1362 $\pm$ 95	532.04 $\pm$ 21.41	583	0.72 $\pm$ 0.02	–
	<b>Co2PO</b>	<b>2018 <math>\pm</math> 61</b>	<b>2054 <math>\pm</math> 57</b>	<b>15.17 <math>\pm</math> 6.46</b>	<b>133</b>	<b>0.30 <math>\pm</math> 0.01</b>	<b>1704000</b>
Safety2x4AntVelocity	MAPPO	1386 $\pm$ 242	704 $\pm$ 37	286.34 $\pm$ 64.61	305	0.50 $\pm$ 0.04	–
	MAPPO-Lag	1038 $\pm$ 89	1315 $\pm$ 51	1.39 $\pm$ 0.52	3	0.00 $\pm$ 0.00	16000
	MACPO	378 $\pm$ 29	493 $\pm$ 22	0.53 $\pm$ 0.28	1	0.00 $\pm$ 0.00	16000
	HAPPO	2041 $\pm$ 405	933 $\pm$ 60	427.80 $\pm$ 99.41	494	0.54 $\pm$ 0.02	–
	<b>Co2PO</b>	<b>1330 <math>\pm</math> 41</b>	<b>1418 <math>\pm</math> 42</b>	<b>13.82 <math>\pm</math> 4.80</b>	<b>133</b>	<b>0.45 <math>\pm</math> 0.04</b>	<b>2810667</b>
Safety4x2AntVelocity	MAPPO	1486 $\pm$ 254	698 $\pm$ 38	341.95 $\pm$ 65.31	383	0.55 $\pm$ 0.03	–
	MAPPO-Lag	1253 $\pm$ 103	1374 $\pm$ 92	1.47 $\pm$ 0.64	4	0.00 $\pm$ 0.00	16000
	MACPO	459 $\pm$ 20	559 $\pm$ 22	1.47 $\pm$ 0.66	2	0.00 $\pm$ 0.00	16000
	HAPPO	1966 $\pm$ 290	749 $\pm$ 42	444.63 $\pm$ 67.31	570	0.61 $\pm$ 0.02	–
	<b>Co2PO</b>	<b>1308 <math>\pm</math> 121</b>	<b>1468 <math>\pm</math> 35</b>	<b>11.34 <math>\pm</math> 7.19</b>	<b>126</b>	<b>0.42 <math>\pm</math> 0.03</b>	<b>2528000</b>
Safety6x1HalfCheetahVelocity	MAPPO	3381 $\pm$ 4	968 $\pm$ 47	805.90 $\pm$ 9.45	826	0.76 $\pm$ 0.02	–
	MAPPO-Lag	1754 $\pm$ 15	1778 $\pm$ 16	2.19 $\pm$ 0.98	4	0.00 $\pm$ 0.00	16000
	MACPO	1159 $\pm$ 70	1236 $\pm$ 17	25.29 $\pm$ 2.43	27	0.01 $\pm$ 0.00	2912000
	HAPPO	3249 $\pm$ 238	1047 $\pm$ 35	739.71 $\pm$ 51.41	838	0.82 $\pm$ 0.01	–
	<b>Co2PO</b>	<b>1829 <math>\pm</math> 79</b>	<b>1894 <math>\pm</math> 55</b>	<b>8.85 <math>\pm</math> 4.65</b>	<b>154</b>	<b>0.29 <math>\pm</math> 0.04</b>	<b>1614667</b>
SafetyAntMultiGoal-0	MAPPO	2.44 $\pm$ 0.93	3.38 $\pm$ 1.73	0.00 $\pm$ 0.00	0	0.00 $\pm$ 0.00	16000
	MAPPO-Lag	6.08 $\pm$ 0.63	7.09 $\pm$ 0.34	0.00 $\pm$ 0.00	0	0.00 $\pm$ 0.00	16000
	MACPO	0.14 $\pm$ 0.29	0.69 $\pm$ 0.05	0.00 $\pm$ 0.00	0	0.00 $\pm$ 0.00	16000
	HAPPO	10 $\pm$ 1	13 $\pm$ 1	0.00 $\pm$ 0.00	0	0.00 $\pm$ 0.00	16000
	<b>Co2PO</b>	<b>8.13 <math>\pm</math> 1.05</b>	<b>10 <math>\pm</math> 1</b>	<b>0.00 <math>\pm</math> 0.00</b>	<b>0</b>	<b>0.00 <math>\pm</math> 0.00</b>	<b>16000</b>
SafetyAntMultiGoal-1	MAPPO	1.66 $\pm$ 0.24	–	78.21 $\pm$ 20.21	137	1.00 $\pm$ 0.00	–
	MAPPO-Lag	1.93 $\pm$ 0.15	–	56.30 $\pm$ 7.64	116	1.00 $\pm$ 0.00	–
	MACPO	-0.12 $\pm$ 0.05	–	76.46 $\pm$ 5.70	121	1.00 $\pm$ 0.00	–
	HAPPO	8.84 $\pm$ 0.85	–	47.38 $\pm$ 12.59	149	1.00 $\pm$ 0.00	–
	<b>Co2PO</b>	<b>2.59 <math>\pm</math> 0.26</b>	<b>–</b>	<b>78.77 <math>\pm</math> 17.02</b>	<b>135</b>	<b>1.00 <math>\pm</math> 0.00</b>	<b>–</b>
SafetyAntMultiGoal-2	MAPPO	1.60 $\pm$ 0.72	–	83.46 $\pm$ 2.57	124	1.00 $\pm$ 0.00	–
	MAPPO-Lag	1.17 $\pm$ 0.21	–	76.27 $\pm$ 16.08	127	1.00 $\pm$ 0.00	–
	MACPO	-0.07 $\pm$ 0.20	–	59.42 $\pm$ 11.00	122	1.00 $\pm$ 0.00	–
	HAPPO	3.72 $\pm$ 1.48	–	86.57 $\pm$ 2.35	151	1.00 $\pm$ 0.00	–
	<b>Co2PO</b>	<b>1.11 <math>\pm</math> 0.03</b>	<b>–</b>	<b>71.27 <math>\pm</math> 0.45</b>	<b>133</b>	<b>1.00 <math>\pm</math> 0.00</b>	<b>–</b>

## B. Effect of Hazard Lookahead Horizon

We study how the hazard lookahead horizon  $H$  used to construct the proactive label  $h_t^i$  in Equation (8) affects final performance. We compare Co2PO variants with  $H \in \{0, 3, 5, 8\}$ , using the same training budget (3,000,000 steps) and evaluation protocol. Table 5 summarizes final-timestep statistics.

Overall, adding a nonzero lookahead yields *consistent* improvements on the coordination-intensive Velocity family: all  $H > 0$  variants reduce average final cost relative to  $H=0$  (while slightly increasing average final reward). The clearest improvement appears at the highest horizon ( $H=8$ ). We also observe that higher horizons increase the number of environments that are cost-compliant at the final checkpoint (from 4/7 to 5/7). Longer lookahead ( $H=8$ ) remains better than  $H=0$  on Velocity costs, but does not further improve the harder MultiGoal settings in our runs (where final costs remain above budget for most methods).

**Table 5. Hazard lookahead horizon  $H$  (final-timestep).** We report averages over the four Velocity environments (HALFCHEETAHVEL and ANTVEL) and the provided averages over all 7 environments. “Feasible envs” counts how many environments satisfy  $C_{\text{final}} \leq d$  at the final checkpoint (budget  $d = 25$ ).

Method	$H$	$\bar{R}_{\text{final}}(\text{Vel}) \uparrow$	$\bar{C}_{\text{final}}(\text{Vel}) \downarrow$	Feasible envs $\uparrow$
Co2PO	0	1607.79	19.34	4/7
Co2PO	3	1621.88	12.30	4/7
Co2PO	5	1639.69	16.32	5/7
Co2PO	8	1644.18	9.42	5/7

**Takeaway.** These results are consistent with the intuition behind proactive labeling: predicting hazards a few steps ahead provides a cleaner trigger for coordination, improving the safety–performance tradeoff on interaction-driven Velocity tasks.

### C. Method Diagram

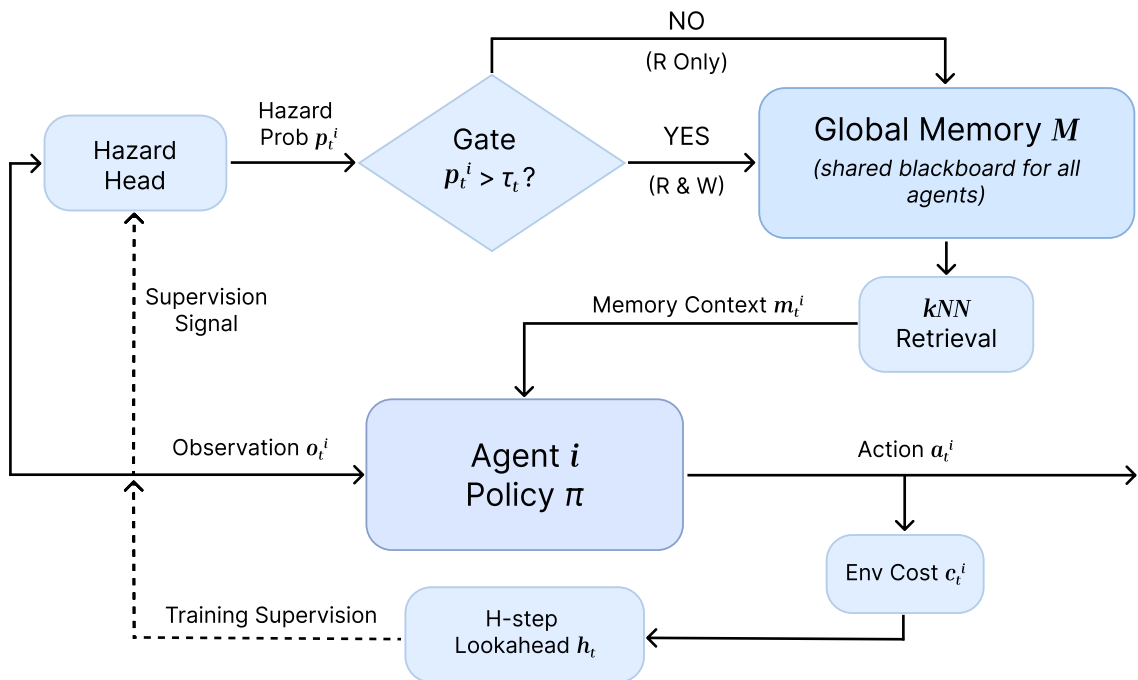


Figure 3. Co2PO Framework Diagram

## D. Detailed Hyperparameters

Table 6. Key method hyperparameters (1/3). Common run settings are in Table 8b.

(a) Co2PO

Hyperparameter	Value
Hidden size	256
MLP layers	2
Discount $\gamma$	0.96
GAE $\lambda$	0.95
PPO clip $\epsilon$	0.2
Target KL	0.016
Update epochs	10
Minibatches	2
Actor LR	$5.0 \times 10^{-4}$
Critic LR	$5.0 \times 10^{-3}$
Entropy coef.	0.0
Max grad norm	10.0
Cost budget $d$	25
Dual init ( $\lambda_0$ )	0.1
Dual step	$5.0 \times 10^{-4}$
Top- $k$ reads ( $k$ )	3
Memory embed dim	64
Hazard lookahead $H$	8
Hazard cost thresh. $\delta$	0.1
Write penalty coef.	0.001
Hazard loss coef.	0.5
Adaptive threshold	True
Init. threshold $\tau$	0.10
Target write rate $\rho^*$	0.05
Threshold LR	0.05
Threshold bounds	[0.05, 0.95]

(b) MAPPO-LAG

Hyperparameter	Value
Hidden size	256
MLP layers	2
Discount $\gamma$	0.96
GAE $\lambda$	0.95
PPO clip $\epsilon$	0.2
Target KL	0.016
Update epochs	10
Minibatches	2
Actor LR	$9.0 \times 10^{-5}$
Critic LR	$5.0 \times 10^{-3}$
Entropy coef.	0.0
Max grad norm	10.0
Cost budget $d$	25
Dual init ( $\lambda_0$ )	0.78
Dual step	$1.0 \times 10^{-5}$

Table 7. Key method hyperparameters (2/3). Common run settings are in Table 8b.

(a) MAPPO

Hyperparameter	Value
Hidden size	256
MLP layers	2
Discount $\gamma$	0.96
GAE $\lambda$	0.95
PPO clip $\epsilon$	0.2
Target KL	0.016
Update epochs	10
Minibatches	2
Actor LR	$9.0 \times 10^{-5}$
Critic LR	$5.0 \times 10^{-3}$
Entropy coef.	0.0
Max grad norm	10.0

(b) MACPO

Hyperparameter	Value
Hidden size	256
MLP layers	2
Discount $\gamma$	0.96
GAE $\lambda$	0.95
PPO clip $\epsilon$	0.2
Target KL	0.016
Update epochs	10
Minibatches	2
Actor LR	$9.0 \times 10^{-5}$
Critic LR	$5.0 \times 10^{-3}$
Entropy coef.	0.0
Max grad norm	10.0
Cost budget $d$	25
Safety $\gamma$	0.09
Step fraction	0.5
CG iters	10
$g$ -step dir coef.	0.1
$b$ -step dir coef.	0.1
Fraction coef.	0.1
EPS	$1.0 \times 10^{-8}$

Table 8. **Key method hyperparameters (3/3)** Common run settings listed here.

(a) HAPPO

Hyperparameter	Value
Hidden size	256
MLP layers	2
Discount $\gamma$	0.96
GAE $\lambda$	0.95
PPO clip $\epsilon$	0.2
Target KL	0.016
Update epochs	10
Minibatches	2
Actor LR	$5.0 \times 10^{-4}$
Critic LR	$5.0 \times 10^{-4}$
Entropy coef.	0.0
Max grad norm	10.0

 (b) **Common run settings (all methods)**

Setting	Value
Total environment steps	3,000,000
Num parallel environments (–num-envs)	16
Num seeds (for uncertainty bands)	3